Received: 14 April 2021 | Revised: 6 July 2021 | Accepted: 8 July 2021

DOI: 10.1002/mbo3.1224

ORIGINAL ARTICLE

MicrobiologyOpen Open Access WILEY

Analysis of N-glycosylation in fungal L-amino acid oxidases expressed in the methylotrophic yeast *Pichia pastoris*

Marc Christian Heß | Marvin Grollius | Valentin Duhay | Simon Koopmeiners | Svenja Bloess | Gabriele Fischer von Mollard

Biochemistry III, Department of Chemistry, Bielefeld University, Bielefeld, Germany

Correspondence
Gabriele Fischer von Mollard, Biochemistry III, Department of Chemistry, Bielefeld University, Universitätsstr. 25, 33615 Bielefeld, Germany
Email: gabriele.mollard@uni-bielefeld.de

Funding information
Deutsche Forschungsgemeinschaft

Abstract

L-amino acid oxidases (LAAOs) catalyze the oxidative deamination of L-amino acids to corresponding α-keto acids. Here, we describe the heterologous expression of four fungal LAAOs in *Pichia pastoris*. *cg*LAAO1 from *Colletotrichum gloeosporioides* and *nc*-LAAO1 from *Neurospora crassa* were able to convert substrates not recognized by recombinant 9His-*hc*LAAO4 from the fungus *Hebeloma cylindrosporum* described earlier thereby broadening the substrate spectrum for potential applications. 9His-*fr*LAAO1 from *Fibroporia radiculosa* and 9His-*la*LAAO2 from *Laccaria amethystine* were obtained only in low amounts. All four enzymes were N-glycosylated. We generated mutants of 9His-*hc*LAAO4 lacking N-glycosylation sites to further understand the effects of N-glycosylation. All four predicted N-glycosylation sites were glycosylated in 9His-*hc*LAAO4 expressed in *P. pastoris*. Enzymatic activity was similar for fully glycosylated 9His-*hc*LAAO4 and variants without one or all N-glycosylation sites after acid activation of all samples. However, activity without acid treatment was low in a variant without N-glycans. This was caused by the absence of a hypermannosylated N-glycan on asparagine residue N54. The lack of one or all of the other N-glycans was without effect. Our results demonstrate that adoption of a more active conformation requires a specific N-glycosylation during biosynthesis.

KEYWORDS
fungi, glycosylation, heterologous expression, L-amino acid oxidases, *Pichia pastoris*

1 | INTRODUCTION

L-amino acid oxidases (LAAOs) are mostly homodimers and contain a non-covalently bound FAD-cofactor. These enzymes catalyze the oxidative deamination of L-amino acids to α-keto acids, ammonia (NH_4^+), and hydrogen peroxide (H_2O_2) (Pollegioni et al., 2013; Yu & Qiao, 2012). LAAOs are found in a wide range of species such as bacteria (Geueke & Hummel, 2002), fungi (Nuutinen & Timonen, 2008), mollusks (Yang et al., 2005), algae (Piedras et al., 1992), fish (Kasai et al., 2010), mammals (Sun et al., 2002) and in venoms of snakes (Bender & Krebs, 1950) or insects (Ahn et al., 2000). LAAOs from snake venoms (*sv*LAAOs) are the best known and best-characterized enzymes, due to the simple purification from venoms (Izidoro et al., 2014). LAAOs contribute to the toxicity of venoms and also show antibacterial, antiviral, antimicrobial, or antitumoral activities in various organisms (Izidoro et al., 2014; Yu & Qiao, 2012). Due to the formation of hydrogen peroxide, they also are used as a defense mechanism (Derby et al., 2018).

LAAOs are of interest for biotechnological applications such as the production of α-keto acids from L-amino acids or D-amino acids from

racemic mixtures of amino acids (Alexandre et al., 2002). However, the recombinant expression of LAAOs with a broad substrate spectrum has been difficult until recently (Pollegioni et al., 2013). Recombinant expression in *E. coli* was successful for 9His-*rs*LAAO1 from the fungus *Rhizoctonia solani* and 6His-*hc*LAAO4 from the fungus *Hebeloma cylindrosporum* (Bloess et al., 2019; Hahn, Neumeister, et al., 2017). Ancestral LAAOs were designed based on different bacterial enzymes and expressed in *E. coli* (Nakano et al., 2019, 2020).

N-glycosylation often plays an essential role in the recombinant expression of proteins. *P. pastoris* can carry out these modifications in contrast to *E. coli*. For LAAOs, these posttranslational modifications are mainly described in *sv*LAAOs. There are two to three N-glycosylation sites described at specific asparagine residues for many *sv*LAAOs (Abdelkafi-Koubaa et al., 2014; Izidoro et al., 2014; Pawelek et al., 2000; Stabeli et al., 2004). N-glycosylations are poorly studied for LAAOs from other organisms such as fungi. The glycosylated LAAO of *Ascomycota Trichoderma harzianum* (*th*LAAO) shows antibacterial effects and also plays a role as an antagonist of *Rhizoctonia solani* (Cheng et al., 2011; Yang et al., 2011).

Recently, we described that 9His-*hc*LAAO4 could be recombinantly expressed as a soluble, active enzyme in *P. pastoris* (Heß et al., 2020). It became N-glycosylated prior to secretion into the culture medium (Heß et al., 2020). Interestingly, 9His-*hc*LAAO4 was much more active than 6His-*hc*LAAO4 expressed in *E. coli*. However, both enzymes reached similar specific activities after acid activation (Bloess et al., 2019, Heß et al., 2020).

Here we show the expression of four additional fungal L-amino acid oxidases as secreted glycosylated proteins in *P. pastoris*. In addition, we characterize N-glycosylation of 9His-*hc*LAAO4 by site-directed mutagenesis. To our understanding, this is the first attempt to analyze the impact of glycosylation on fungal LAAOs.

2 | RESULTS

2.1 | Expression of fungal LAAOs in *P. pastoris*

Recently, we were able to express 9His-*rs*LAAO1 and 9His-*hc*LAAO4 as active proteins (Hahn, Neumeister, et al., 2017, Heß et al., 2020). They do not convert all proteinogenic L-amino acids even though both enzymes have a fairly broad substrate spectrum. Databases were searched for fungal sequences encoding predicted LAAOs. We focused on the small number of LAAOs with predicted ER-signal sequences with the rationale that a naturally secreted protein may offer a higher chance of active expression as a secreted protein in *P. pastoris* (Table 1). A LAAO from *Laccaria amethystina* (*la*LAAO2) was selected as a more closely related enzyme (52% amino acid identity with *hc*LAAO4).

To explore more divergent enzymes, a predicted LAAO from the *Ascomycota Colletotrichum gloeosporioides* (35% amino acid identity) was selected. The purification of a highly active LAAO from the *Ascomycota Neurospora crassa* and its cloning was reported (Niedermann & Lerch, 1990) but it has not been expressed heterologously. *nc*LAAO1 is very different from *hc*LAAO4 (23% amino acid identity). In addition, *fr*LAAO1 was expressed as an enzyme without an ER-signal sequence from the *Basidiomycota Fibroporia radiculosa*. The synthetic genes lack the information for ER-signal sequences and were codon-optimized for expression in *P. pastoris*. Initially, these putative LAAOs were expressed in *E. coli* as 6His- or maltose-binding protein fusion proteins. However, the fusion proteins were either completely insoluble or the low amounts of soluble MBP-fusion proteins were inactive as in the case of MBP-*cg*LAAO1 (Figure A1). The genes coding for these LAAOs were cloned into the *P. pastoris* expression vector pPIC9K, which encodes the prepro-sequence of the α-mating factor of *S. cerevisiae* as an N-terminal ER import signal sequence. Linearized plasmids were integrated into the *HIS4* locus of *P. pastoris* SMD1163. Clones were selected according to (Scorer et al., 1994). Expression was induced in a medium at pH 6.0 with 1% methanol at 15°C and samples were taken every 24 h for 96 h (Figure 1).

Two LAAOs, 9His-*nc*LAAO1 (*nc*: *Neurospora crassa*, Figure 1a) and 9His-*la*LAAO2 (*la*: *Laccaria amethystine*, Figure 1d), could be detected in western blots of supernatants after an expression for 48 h. 9His-*fr*LAAO1 (*fr*: *Fibroporia radiculosa*) and 9His-*cg*LAAO1 (*cg*: *Colletotrichum gloeosporioides*) were visible after 72 h (Figure 1b,c). 9His-*fr*LAAO1 was not further characterized due to low expression levels. Only 0.8 U of purified 9His-*la*LAAO2 were obtained per 1 liter of culture due to poor binding to the column material. The substrate spectrum of 9His-*la*LAAO2 was similar to that of 9His-*hc*LAAO4. 9His-*cg*LAAO1 was expressed at 360 U L^{-1}, but only 34 U L^{-1} of the purified enzyme were obtained due to poor binding to the column

TABLE 1 Overview of expressible fungal L-amino acid oxidases

Original organism		Division	ER-signal sequence	Put. *N*-sites	Glycosylated	Predicted MW (kDA)	% sequence identity	Yield (U L^{-1})	
								SN	Purified
H. cylindrosporum	LAAO4	B	+	4	+	68.6	100	180[a]	180[a]
L. amethystina	LAAO2	B	+	6	+	70.9	52	n. d.	0.8
F. radiculosa	LAAO1	B	–	2	+	65.0	35	n. d.	n. d.
C. gloeosporioides	LAAO1	A	+	10	+	67.9	35	360	34
N. crassa	LAAO1	A	+	10	+	64.2	23	30	9

Abbreviations: A, *Ascomycota*; B, *Basidiomycota*; n.d., not determined; SN, culture supernatant.

[a]Heß et al., 2020.

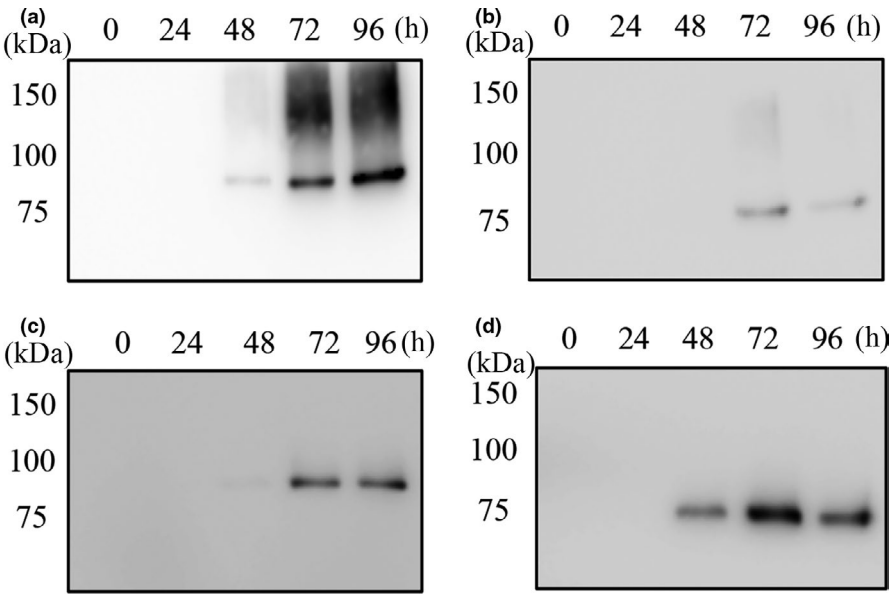

FIGURE 1 Expression of four fungal LAAOs in *P. pastoris*. Genes encoding fungal LAAOs were integrated into the *HIS4* locus of *P. pastoris* SMD1163. Expression was induced in 50 ml BMMY medium pH 6.0 with 1% methanol added every 24 h at a temperature of 15°C for 96 h. A sample was taken every 24 h and the supernatant was analyzed with western blotting. (a) 9His-*nc*LAAO1 (MCH13). (b) 9His-*fr*LAAO1 (MCH17). (c) 9His-*cg*LAAO1 (MCH5). (d) 9His-*la*LAAO2 (MCH8)

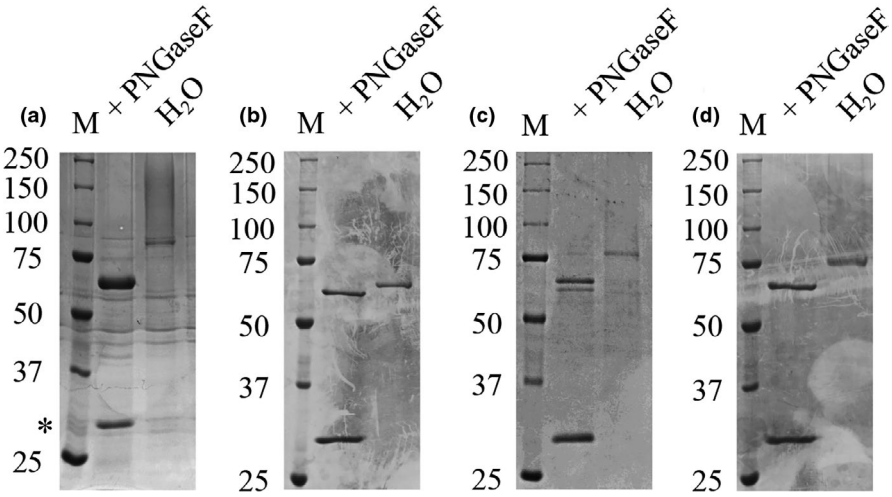

FIGURE 2 N-glycosylation of four fungal LAAOs expressed in *P. pastoris*. Deglycosylation of purified fungal LAAOs was achieved with PNGaseF overnight at 37°C. Deglycosylated enzymes and controls treated with H_2O were separated by SDS-PAGE. The gels were stained with Coomassie. * PNGaseF (a) 9His-*nc*LAAO1 (MCH13). (b) 9His-*fr*LAAO1 (MCH17). (c) 9His-*cg*LAAO1 (MCH5). (d) 9His-*la*LAAO2 (MCH8)

material. 9His-*cg*LAAO1 had a broad substrate spectrum (Table A2) including L-tryptophan, which is a poor substrate for 9His-*hc*LAAO4. K_m values were around 1 mM and v_{max} values around 10 U mg^{-1} for the best substrates L-glutamine, L-leucine, and L-methionine (Table A3). 9 U L^{-1} of 9His-*nc*LAAO1 could be obtained from culture supernatants with 30 U L^{-1}. The very broad substrate spectrum of 9His-*nc*LAAO1 includes amino acids not or poorly converted by other recombinant fungal LAAOs such as L-valine, L-serine, L-threonine, L-aspartic acid, and L-phenylglycine at a substrate concentration of 10 mM (Table A4). N-α-acetyl-L-lysine was a very good substrate indicating that the enzyme could also oxidase the ε-amino group. The ability to oxidize N-α-acetyl-L-lysine in addition to N-ε-acetyl-L-lysine and many L-amino acids has also been observed for a LAAO isolated from *Rhodococcus* sp. AIU Z-35-1 (Isobe & Nagasawa, 2007). K_m values were below or at 10 µM and v_{max} values around 1 U mg^{-1} for the best substrates L-arginine, L-phenylalanine, and L-leucine (Table A5). However, activities were lower at a substrate concentration of 10 mM than at 0.1 mM for these and good substrates such as L-tryptophan and L-histidine (Table A4). This inhibition was much stronger for L-arginine (specific activity 0.13 U mg^{-1}) than for L-phenylalanine (0.53 U mg^{-1}, Figure A2b,c). Substrates with a high K_m value such as L-isoleucine were not affected (Figure A2a). As 9His-*rs*LAAO1 was activated by SDS (Hahn, Hertle, et al., 2017) and 9His-*hc*LAAO4 by exposure to acidic pH (Heß et al., 2020) we determined the influence of these two treatments and pH 9.0 on 9His-*cg*LAAO1 and 9His-*nc*LAAO1. The activity of 9His-*nc*LAAO1 increased slightly after these treatments (Figure A3a) while 9His-*cg*LAAO1 was not influenced (Figure A3b).

2.2 | Proof of N-glycosylation for fungal LAAOs and analysis of activity after deglycosylation

All four expressed LAAOs were detected at a higher position in western blots (Figure 1) than expected from the predicted molecular weight (Table 1). These enzymes contain between 2 and 10 possible

N-glycosylation sites predicted by the NetNGlyc 1.0 webserver (Table 1). LAAOs purified from culture medium were deglycosylated with PNGaseF or incubated with water as controls (Figure 2).

A band at the position expected for the theoretical molecular weight of these four enzymes (determined by ExPASy ProtParam tool, see also Table 1) was obtained after the addition of PNGaseF (Figure 2, lanes +PNGaseF). Two bands were detected after deglycosylation of 9His-*cg*LAAO1 (Figure 2c) suggesting that it was only partially deglycosylated.

In the first set of experiments, the impact of deglycosylation on activity was determined for 9His-*nc*LAAO1 and 9His-*cg*LAAO1 (Figure 3) according to (Heß et al., 2020). The activity was measured with a coupled peroxidase/*o*-dianisidine assay. Deglycosylation of 9His-*nc*LAAO1 with PNGaseF overnight at 37°C did not alter activity compared to controls with additions of water (Figure 3a, +PNGaseF, 37°C: 0.43 ± 0.06 U mg^{-1}; H_2O, 37°C: 0.49 ± 0.07 U mg^{-1}; H_2O, 4°C: 0.37 ± 0.11 U mg^{-1}). This suggests that N-glycosylation is not essential for activity but may support the proper folding of the enzyme during biosynthesis. The activity of 9His-*cg*LAAO1 was reduced by incubation overnight at 37°C (Figure 3b).

2.3 | Site-directed mutagenesis of 9His-*hc*LAAO4

We have already shown that deglycosylation does not reduce the activity of 9His-*hc*LAAO4 expressed in *P. pastoris* (Heß et al., 2020). 6His-*hc*LAAO4 expressed in *E. coli* has a much lower specific activity (2 U mg^{-1}) compared to 9 U mg^{-1} by 9His-*hc*LAAO4 expressed in *P. pastoris* (Bloess et al., 2019, Heß et al., 2020). However, similar specific activity is reached after acid activation. This means that the maximal activity is not affected by glycosylation. Therefore, glycosylation may have a role during biosynthesis resulting in a stable, more active conformation.

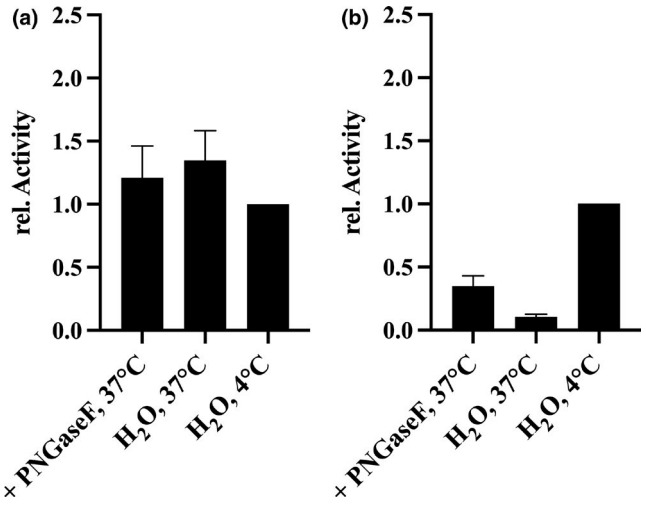

FIGURE 3 Activity of two fungal LAAOs after deglycosylation. Enzymatic activity was assayed with peroxidase and *o*-dianisidine in TEA buffer pH 7.0. To determine the impact of the 37°C incubation, an untreated control sample was stored at 4°C. Data were normalized to the 4°C control. Data are means of three independent experiments; error bars represent standard deviations. (a) 9His-*nc*LAAO1 (MCH13). Substrate: 10 mM L-leucine ethyl ester. (b) 9His-*cg*LAAO1 (MCH5). Substrate: 10 mM L-glutamine

*hc*LAAO4 has four predicted N-glycosylation sites according to NetNGlyc 1.0 webserver at amino acid residues N54, N164, N193, N331.

These asparagine residues were changed to alanine residues. Single mutants (N54A, N164A, N193A, N331A), a triple mutant (N164A N193A N331A), and the mutant without putative N-glycosylation sites (ΔN-Glyc.) were expressed and purified as described in experimental procedures.

The enzyme variants were analyzed via western blotting (Figure 4). The ΔN-Glyc. mutant enzyme was detected at the same position as 6His-*hc*LAAO4 expressed in *E. coli* and the deglycosylated 9His-*hc*LAAO4 indicating that there was no additional posttranslational modification present in the enzyme expressed in *P. pastoris* (Heß et al., 2020). All single mutant enzymes (N54A, N164A, N193A, and N331A) were detected at a lower position than the wild-type enzyme (Wt). These results suggest that 9His-*hc*LAAO4 carries N-glycans at all four putative N-glycosylation sites. The N54A mutant had a lower position than the other single mutants. The N54A and the ΔN-Glyc. variants could be detected as clear bands, whereas all other single mutants, the N164A N193A N331A triple mutant as well as the wild-type enzyme showed a diffuse band (Figure 4). This could be due to a heterogenous hyperglycosylation on N54 and a more frequently observed N-glycosylation with $Man_{8\text{-}9}GlcNAc_2$ (Bretthauer & Castellino, 1999) at the three other N-glycosylation sites. Furthermore, the band of the N54A mutant was on the same height as the upper band of the partially deglycosylated 9His-*hc*LAAO4 (Figure 6, lane +PNGaseF, 37°C, and N54A) indicating that the N-glycan at N54 was more efficiently removed than the other N-glycans.

The activity was determined using a coupled peroxidase/*o*-dianisidine assay with 10 mM L-glutamine. For comparisons, we used 6His-*hc*LAAO4 expressed in *E. coli* (*E. coli* Wt) (Bloess et al., 2019) and fully glycosylated 9His-*hc*LAAO4 expressed in *P. pastoris* (Wt).

Among the untreated enzymes with L-alanine in one N-glycosylation site, the N54A exchange showed the biggest reduction of activity (Figure 5 and Table A6). The specific activity of the N54A mutant enzyme was 2.8-fold lower in comparison to the wild-type enzyme (4.9 U mg^{-1} to 14.1 U mg^{-1}). In contrast, small reductions in activity could be detected in proteins without one of the other N-glycosylation sites or with N54 as the only remaining site (13.4 U mg^{-1} to 11.6 U mg^{-1}, Figure 5 and Table A6). These data suggest that N54 carries the most important N-glycan for basal activity of 9His-*hc*LAAO4. The enzyme without N-glycosylation sites (ΔN-Glyc.) showed nearly the same activity as 6His-*hc*LAAO4 expressed in *E. coli* (2.4 U mg^{-1} to 1.1 U mg^{-1} for *E. coli* Wt). However, the specific activities reached similar values for all enzyme variants expressed in *P. pastoris* after pH3 activation (39.6 U mg^{-1} to 44.5 U mg^{-1} compared to 42.8 U mg^{-1} for the wild-type enzyme). Acid-activated 6His-*hc*LAAO4 expressed in *E. coli* reached 33.3 U mg^{-1} (Figure 5 and Table A6).

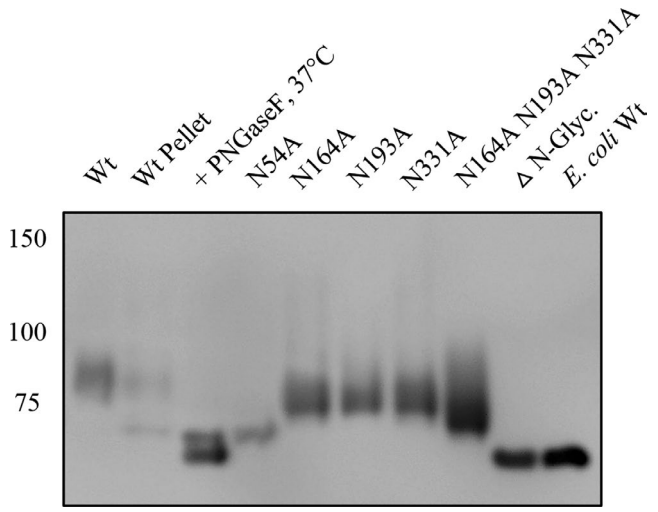

FIGURE 4 9His-*hc*LAAO4 contained four N-glycans after expression in *P. pastoris*. To analyze glycosylation in *P. pastoris* 9His-*hc*LAAO4 wild type (Wt), the pellet of a 9His-*hc*LAAO4 expression (Wt Pellet), the deglycosylated wild type (+PNGaseF, 37°C), the single mutants (N54A, N164A, N193A, N331A), the triple mutant (N164A N193A N331A), and the quadruple mutant (ΔN-Glyc.) were analyzed and compared to the non-glycosylated 6His-*hc*LAAO4 wild type expressed in *E. coli* (*E. coli* Wt). A sample of 9His-*hc*LAAO4 was deglycosylated overnight at 37°C with PNGaseF. Mutations were inserted successively by site-directed mutagenesis. Purified enzymes were separated by SDS-PAGE and analyzed via western blotting

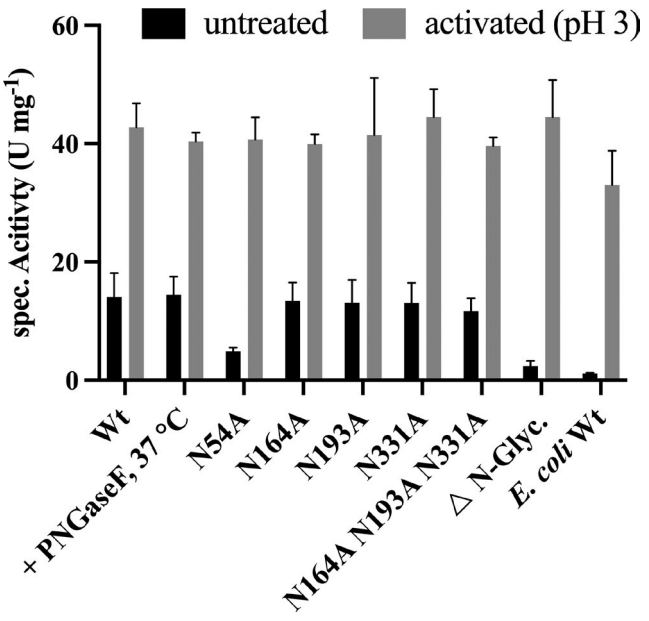

FIGURE 5 Effect of N-glycosylation on 9His-*hc*LAAO4 activity. Mutant enzymes were expressed in *P. pastoris* and purified from the culture medium. Activities were measured with a coupled peroxidase/*o*-dianisidine assay with L-glutamine as a substrate for untreated variants of 9His-*hc*LAAO4 and acid-activated (pH 3) variants. Controls were glycosylated wild type from *P. pastoris* (Wt), deglycosylated 9His-*hc*LAAO4 (+PNGaseF, 37°C), and non-glycosylated wild type expressed in *E. coli* (*E. coli* Wt). Data are means of three independent experiments; error bars represent standard deviations

To investigate the hydrodynamic radius of the enzymes we performed analytical size exclusion chromatography (Figure 6). The untreated wild-type enzyme (Wt, black line) eluted at a volume of 11.45 ml, which corresponds to 216 kDa. The enzyme without N-glycosylation sites ΔN-Glyc. (13.46 ml) behaved very similar to the *E. coli* expressed 6His-*hc*LAAO4 (13.19 ml, Figure 6a). The PNGaseF treated wild type 9His-*hc*LAAO4 (+PNGaseF, 37°C) eluted at 12.07 ml (159 kDa) indicating that the partial deglycosylation reduced the hydrodynamic radius. Acid activation shifted the *E. coli* expressed 6His-*hc*LAAO4 to 12.23 ml in comparison to the untreated enzyme (13.19 ml) as already described (Bloess et al., 2019). Expressed in *P. pastoris* neither wild type nor ΔN-Glyc. enzyme similarly changed mobility upon acid activation (11.25 ml and 13.10 ml, Figure 6b).

Finally, we analyzed whether glycosylation affected temperature stability. Acid-activated enzymes were incubated at 70°C for 10–120 min before the activity assay at 30°C. Fully glycosylated 9His-*hc*LAAO4 lost only 10% of its activity as described before (Heß et al., 2020). The enzyme lacking all four N-glycosylation sites (ΔN-Glyc) was inactivated by 60 min (Figure 7). Inactivation was already observed at 30°C. Enzyme variants with asparagine to alanine exchanges in one N-glycosylation site were slightly less stable than the wild-type enzyme. All variants were quickly inactivated at 80°C.

3 | DISCUSSION

Here we describe that four fungal L-amino acid oxidases could not be expressed as active proteins in *E. coli* but were successfully expressed as secretory proteins in the yeast *P. pastoris*. All of these enzymes were N-glycosylated in *P. pastoris* even though only three of them contain predicted ER-signal sequences indicating that they are secretory proteins originally. Likely, the N-glycosylation improved the folding and solubility of these enzymes as carbohydrates are very hydrophilic. A similar observation was made for the snake venom LAAO from *Calloselasma rhodostoma* (*cr*LAAO, Kommoju et al., 2007). While expression in *E. coli* resulted in inclusion bodies, *cr*LAAO was expressed as an active, N-glycosylated enzyme in *P. pastoris*. N-glycosylation is required for solubility of this LAAO as deglycosylation of *cr*LAAO expressed in *P. pastoris* and isolated from snake venom resulted in precipitation of the protein and inactivation. Deglycosylation did not decrease the activity of 9His-*nc*LAAO1 as well as 9His-*hc*LAAO4 (Heß et al., 2020). 9His-*cg*LAAO1 was partially inactivated due to the incubation at 37°C overnight but did not lose activity completely. These data indicate that N-glycosylation is not a prerequisite for solubility for these fungal LAAOs. Deglycosylation did not influence the activity of LAAOs isolated from snake venom of different species of *Bothrops*: *Bothrops pirajai* (Izidoro et al., 2006),

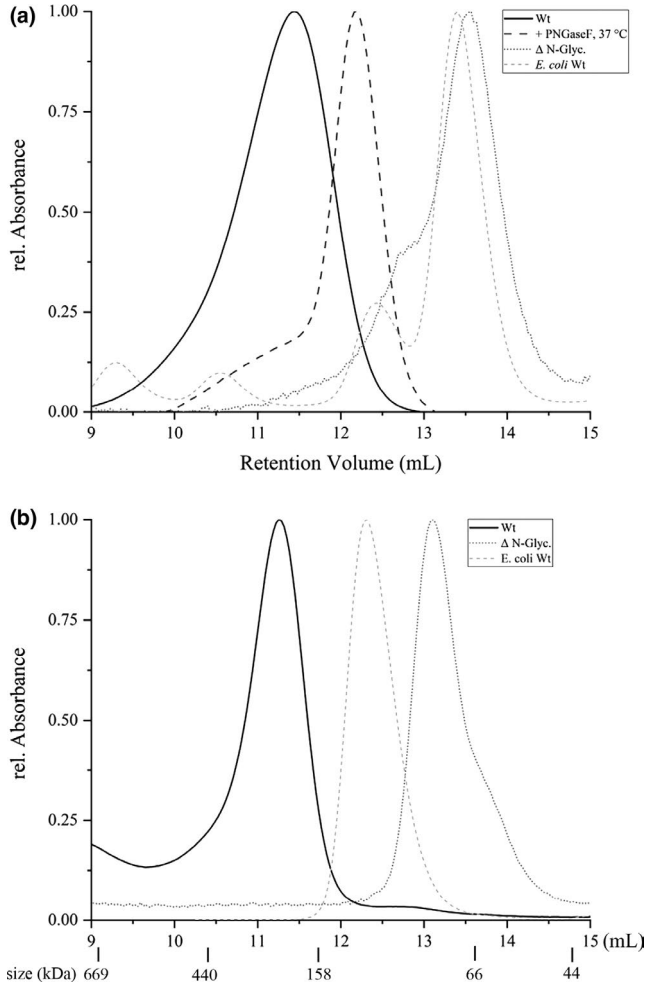

FIGURE 6 Hydrodynamic radius dependent on glycosylation and acid activation. *P. pastoris* wild type (Wt), deglycosylated 9His-*hc*LAAO4 (+PNGaseF, 37°C), 9His-*hc*LAAO4 without N-glycans (ΔN-Glyc.) and non-glycosylated wild type from *E. coli* (*E. coli* Wt) were analyzed by size exclusion chromatography. Glycosylation resulted in a larger hydrodynamic radius. Acid activation (b) increased the hydrodynamic radius for 6His-*hc*LAAO4 from *E. coli* (*E. coli* Wt) compared to untreated samples (a)

Bothrops pauloensis (Rodrigues et al., 2009), *Bothrops alternatus* (Stabeli et al., 2004); and *Cerastes cerastes* (Abdelkafi-Koubaa et al., 2014). Glycosylation in fungal LAAOs has been rarely studied. It has been shown that the LAAO isolated from the *Agaricomycetes* fungus *Amanita phalloides* (*Ap*LAO) is N-glycosylated (Sabotic et al., 2020). However, the effect of deglycosylation on activity was not analyzed.

9His-*cg*LAAO1 is of potential interest for biotechnological applications because it can convert L-tryptophan with higher specific activity compared to 9His-*rs*LAAO1 or 9His-*hc*LAAO4 (Hahn, Neumeister, et al., 2017, Heß et al., 2020). However, v_{max} for the best substrates is lower for 9His-*cg*LAAO1 than for 9His-*hc*LAAO4 (13 U mg^{-1} compared to 30 U mg^{-1}). 9His-*nc*LAAO1 has low v_{max} (1 U mg^{-1}) and very low K_m values in the range of 5–10 μM for the best substrates, which is about 100-fold lower than K_m values for the three other fungal LAAOs studied. In addition, the activity of 9His-*nc*LAAO1 is inhibited at 10 mM substrate concentration for many L-amino acids. On the other hand, 9His-*nc*LAAO1 converts substrates, which are not accepted by the other three fungal LAAOs such as L-valine, L-serine, L-threonine, L-aspartic acid, and L-phenylglycine. 9His-*nc*LAAO1 and 9His-*cg*LAAO1 are not activated by acidic pH or by SDS in contrast to 9His-*rs*LAAO1 and 9His-*hc*LAAO4.

Site-directed mutagenesis was used to analyze the roles of the different N-glycans in detail. In contrast to *S. cerevisiae*, *P. pastoris* contains mostly $Man_{8\text{-}9}GlcNAc_2$-glycans but is also capable to synthesize N-glycans with more mannose residues (Bretthauer & Castellino, 1999). The diffuse band of 9His-*hc*LAAO4 and its N164A, N193A, N331A and N164A N193A N331A variants (Figure 4) suggest the occurrence of a hypermannosylated N-glycan. A sharp band appeared due to the removal of the N-glycosylation site at N54. These data indicate N54 is hypermannosylated while N164, N193, and N331 carry $Man_{8\text{-}9}GlcNAc_2$-glycans.

Similar specific activation was reached after acid activation regardless of the removal of one or more N-glycosylation sites (Figure 5). These data indicate that activation and maintenance of the active conformation did not depend on N-glycosylation.

The N-glycan at N54 had the highest impact on untreated activity (Figure 4 and Table A6). The N54A exchange reduced the specific activity to 4.9 U mg^{-1} while removal of one or all of the three other N-glycosylation sites did not change the specific activity or had little impact. The specific activity was even lower in the absence of all N-glycans (2.4 U mg^{-1}). Deglycosylation of 9His-*hc*LAAO4 did not reduce the specific activity of the untreated or acid-activated enzyme (Figure 5 and (Heß et al., 2020)). These data suggest that *hc*LAAO4 adopts a conformation of low activity if synthesized without N-glycans. The N-glycan at N54 induces folding into a conformation of intermediate activity during biosynthesis. Once this conformation is formed it is not sensitive to the removal of N-glycans by deglycosylation. The most active conformation can be reached by acid activation independent of N-glycans.

Activation by acid (6His-*hc*LAAO4, Bloess et al., 2019) or SDS (9His-*rs*LAAO1, Hahn, Hertle, et al., 2017) after expression in *E. coli* results in a conformational change, which can be detected as an increase in size by size exclusion chromatography. When expressed in *P. pastoris*, 9His-*hc*LAAO4 had a higher hydrodynamic radius than 6His-*hc*LAAO4 expressed in *E. coli*, which was reduced by deglycosylation (Figure 6). 9His-*hc*LAAO4 did not elute at a lower retention volume after acid activation. The untreated ΔN-Glyc.-protein eluted at a retention volume similar to the untreated 6His-*hc*LAAO4 expressed in *E. coli* (*E. coli* Wt) consistent with the identical mobility in SDS-PAGE (Figure 4). We did not observe a change in the elution volume of the ΔN-Glyc.-protein after acid treatment. This behavior may point toward differences in activation of the ΔN-Glyc.-protein expressed in *P. pastoris* and 6His-*hc*LAAO4 expressed in *E. coli*.

Temperature stability was greatly reduced in the ΔN-Glyc.-enzyme. These data indicate that N-glycosylation contributes to the temperature stability of 9His-*hc*LAAO4 expressed in *P. pastoris*. However, 6His-*hc*LAAO4 expressed in *E. coli* is not inactivated at

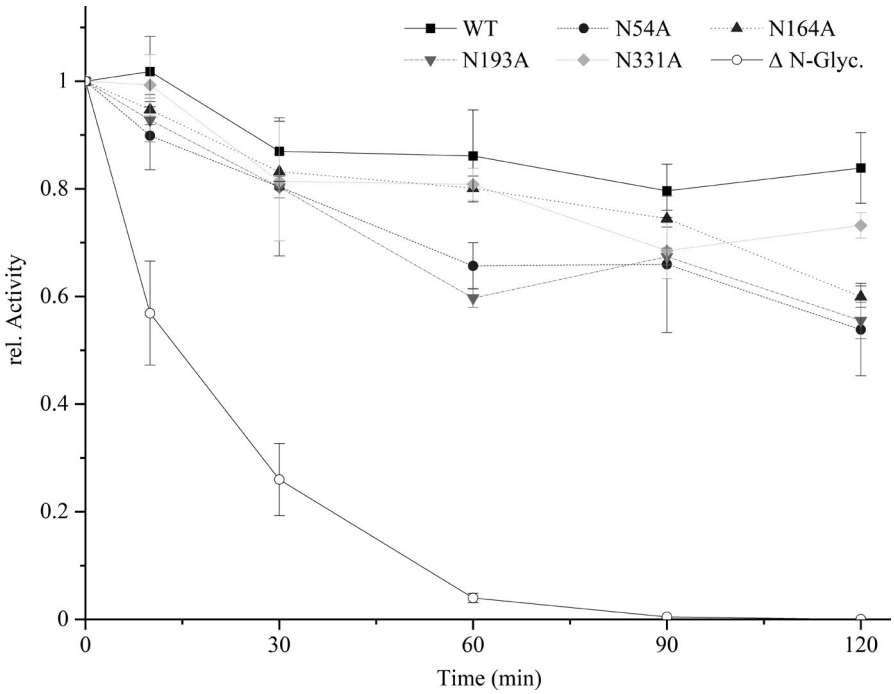

FIGURE 7 Lower temperature stability of 9His-*hc*LAAO4 without N-glycosylation sites. Purified 9His-*hc*LAAO4 and variants with asparagine to alanine exchanges in one or all four N-glycosylation sites were incubated at 70°C for the indicated periods. Enzymatic activity was assayed with peroxidase and *o*-dianisidine in TEA buffer pH 7.0 at 30°C with L-glutamine as substrate. Data were normalized to a control without preincubation. Data are means of three independent experiments; error bars represent standard deviations

70°C even though it is not glycosylated (Heß et al., 2020). Enzymatic deglycosylation of 9His-*hc*LAAO4 overnight at 37°C does not inactivate the enzyme (Heß et al., 2020). Four hydrophilic asparagine residues were replaced with less hydrophilic alanine residues on the surface of the ΔN-Glyc.-enzyme. These changes in the surface may also destabilize the enzyme.

Our results contribute to understanding the effect of glycosylation at fungal LAAOs and will help for further biochemical characterizations of fungal LAAOs.

4 | EXPERIMENTAL PROCEDURES

4.1 | Amplification and cloning of LAAOs

The synthetic genes (GenBank accession numbers MW752153 (*cg*LAAO1), MW752154 (*nc*LAAO1), MW752155 (*la*LAAO2), and MW752156 (*fr*LAAO1)) of the LAAOs (Table 1) were amplified with the forward primers in Table A1 introducing an EcoRI recognition site (underlined sequence) followed by a 9His-tag (bold) upstream of the LAAO coding sequence. The reverse primers in Table A1 contained the stop-Codon (bold) and the NotI site (underlined sequence). The PCR products were cloned in an intermediate step into pGEM-TEasy (Promega), digested with EcoRI and NotI, and ligated into the EcoRI and NotI digested pPIC9K (Invitrogen), which encodes the pre-pro-sequence of α-mating factor. The cloning of 9His-*hc*LAAO4 (GenBank accession number MH751433, (Bloess et al., 2019)) was briefly described (Heß et al., 2020). The four N-glycosylation sites of *hc*LAAO4 predicted by NetNGlyc 1.0 webserver were changed into alanine residues one after the other via overlap PCR as described (Heß et al., 2020). For the expression in *E. coli*, LAAO-genes were inserted in pET28b-vector (Novagen) encoding an N-terminal 6His-tag via restriction sites NdeI and NotI according to (Bloess et al., 2019).

4.2 | Genome integration into *P. pastoris* and selection of clones

Genomic integration was carried out according to (Heß et al., 2020). Cells of *P. pastoris* SMD1163 yeast strain (Invitrogen) were spheroplasted and linearized plasmids were transformed via electroporation (linearization with SalI for integration into the *HIS4* locus). After electroporation, 1 M ice-cold sorbitol was added immediately and the cells were spread on MD-His agar plates (0.17% yeast nitrogen base, 0.4 μg L^{-1} biotin, 2% glucose, amino acid mix (50 mg L^{-1} each of L-glutamic acid, L-methionine, L-lysine, L-leucine, L-isoleucine), 1.5% Agar). Plates were incubated at 30°C for 2 days as described (Wu & Letchworth, 2004). The selection was performed according to (Scorer et al., 1994) on YEPD-agar-plates with increasing concentration of G-418 (Geneticin, Calbiochem) (1 mg ml^{-1}, 2.5 mg ml^{-1}, 5 mg ml^{-1}, 7.5 mg ml^{-1}, 10 mg ml^{-1}). Plates were cultured at 30°C for several days.

4.3 | Analysis of expression of LAAOs

Clones were screened for the highest LAAO expression after induction with methanol as described (Heß et al., 2020). For this, clones were cultivated overnight at 30°C in 20 ml BMGY medium (2% peptone, 1% yeast extract, 100 mM potassium phosphate pH 6.0, 1.34% yeast nitrogen base, 0.4 μg ml^{-1} biotin, 1% glycerol). 50 ml

BMMY medium (2% peptone, 1% yeast extract, 100 mM potassium phosphate pH 6.0, 1.34% yeast nitrogen base, 0.4 μg ml^{-1} biotin, 1% methanol) was inoculated with 1 OD600 of cells. Expression was performed at 15°C and 190 rpm for 96 h. Methanol was added every 24 h to a final concentration (v/v) of 1%. Every 24 h a sample was taken and centrifuged (4°C, 4600 g, 5 min). 30 μl of the supernatants were analyzed via western blotting.

4.4 | Expression of LAAOs

Cells were cultivated in 20 ml BMGY medium at 30°C for at least 16 h, as described in Heß et al., 2020. Cells were centrifuged and diluted into 500 ml BMMY medium for 72 h at 15°C. Methanol was added every 24 h to a final concentration (v/v) of 1%. After centrifugation of cells (4°C, 4,600 g, 10 min), the supernatants (medium) with secreted LAAOs were stored at 4°C and used for purification of the enzymes. Expression in *E. coli* Arctic express (DE3) was done according to (Bloess et al., 2019) in 250 ml LB-broth (10 g L^{-1} bacto tryptone, 5 g L^{-1} yeast extract, 5 g L^{-1} NaCl, 1 g L^{-1} glucose) or 500 ml HSG-medium (13.5 g L^{-1} soy peptone, 7 g L^{-1} yeast extract, 14.9 g L^{-1} glycerol (99%), 2.5 g L^{-1} NaCl, 2.3 g L^{-1} K_2HPO_4, 1.5 g L^{-1} KH_2PO_4, 0.14 g L^{-1}, $MgSO_4 \cdot H_2O$, pH 7.4) with 50 μg ml^{-1} kanamycin and 25 μg ml^{-1} gentamycin at 11°C and was induced by 0.05 mM IPTG.

4.5 | Purification of the secreted LAAO

Purification was performed at 4°C as described (Heß et al., 2020). The supernatant with the secreted LAAO was loaded onto a Ni^{2+}-NTA resin. The flow-through was collected, mixed, and reloaded onto the Ni^{2+}-NTA resin via a peristaltic pump for 24 h with a flow velocity of 1 ml min^{-1}. The column was washed with 10 column volumes (cv) of His-washing buffer (50 mM Na_2HPO_4 pH 7.0, 300 mM NaCl and 20 mM imidazole). LAAO was eluted with 10 ml His buffer (50 mM Na_2HPO_4 pH 7.0, 300 mM NaCl and 500 mM imidazole). The enzyme was concentrated via ultrafiltration (Vivaspin 6 30.000 MWCO, Sartorius), rebuffered into HEPES buffer pH 7.0 (100 mM HEPES, 150 mM NaCl), and stored at 4°C. Size exclusion chromatography was performed according to Bloess et al., 2019 with an Ettan LC (GE Healthcare Life Sciences, Chicago, IL, USA) on a Superdex® 200 *Increase* 10/300 GL column (GE Healthcare Life Sciences, Chicago, IL, USA).

4.6 | Enzymatic assay

Enzymatic activity of LAAOs was measured using a coupled peroxidase/*o*-dianisidine assay with 10 mM L-amino acid as described (Hahn, Neumeister, et al., 2017). The initial rate of H_2O_2 production was measured. A standard assay mixture contained 10 mM L-glutamine (for 9His-*hc*LAAO4 or 9His-*cg*LAAO1) or L-leucine ethyl ester (for 9His-*nc*LAAO1), 50 mM TEA/HCl buffer (pH 7.0), 0.2 mg ml^{-1} of *o*-dianisidine, 5 U ml^{-1} peroxidase and LAAO in limiting amounts (0.75–2 μg in a 200 μl assay). Absorption was measured in 96-well plates at 30°C in a Tecan Spark microplate reader at 436 nm. One unit was defined as the amount of enzyme that catalyzes the conversion of 1 μmol L-amino acid per minute. To determine the impact of various conditions on the activity, enzymes were preincubated with 1.5 mM SDS or different pH values (pH 3.0, 4.5, 7.0, 9.0) for 10 min and then measured under standard conditions. Initial velocities of H_2O_2 production were determined with different L-amino acid concentrations between 0.02 and 20 mM for 9His-*cg*LAAO1 or 9His-*nc*LAAO1. K_m and v_{max} values were calculated from Hanes-Woolf plots.

4.7 | Deglycosylation of LAAOs

Deglycosylation was performed by PNGaseF (NEB). To analyze enzymatic activity the PNGaseF mixture contained 100 mM EDTA pH 8.0, 100 mM Tris-HCl pH 8.0, 1 μM PMSF in DMSO, 1% (w/v) CHAPS and 500 U PNGaseF. The digestion was done overnight at 37°C. As controls, PNGaseF was replaced with water, and samples were incubated at 37°C or 4°C overnight. For SDS-PAGE the mixture containing 5 μg of glycoprotein and 1 μl 10× glycoprotein denaturing buffer (NEB) in a total of 10 μl was heated at 95°C for 10 min. After adding 2 μl 10× GlycoBuffer 2 (NEB), 2 μl 10% NP40 (NEB), 5 μl H_2O und 500 U PNGaseF, the mixture was incubated at 37°C and 300 rpm for 1 h.

ACKNOWLEDGMENTS

We thank Annamaria Latus and Felix Höhner for excellent technical support. Funding was supplied by Bielefeld University and Deutsche Forschungsgemeinschaft (DFG, initial funding for CRC 1416).

CONFLICT OF INTEREST

None declared.

AUTHOR CONTRIBUTIONS

Marc Christian Heß: Conceptualization (supporting); Data curation (lead); Investigation (lead); Visualization (lead); Writing-original draft (equal); Writing-review & editing (supporting). **Marvin Grollius:** Investigation (supporting). **Valentin Duhay:** Investigation (supporting). **Simon Koopmeiners:** Investigation (supporting); Writing-review & editing (supporting). **Svenja Bloess:** Investigation (supporting); Writing-review & editing (supporting). **Gabriele Fischer von Mollard:** Conceptualization (lead); Data curation (supporting); Supervision (lead); Visualization (supporting); Writing-original draft (equal); Writing-review & editing (lead).

ETHICS STATEMENT

Work with recombinant DNA has been performed according to national requirements (Dt-55.3.5-5/94-Bi, Anlage Nr. 412).

DATA AVAILABILITY STATEMENT

Data associated with this article can be found at PUB (Publikationen an der Universität Bielefeld) under https://doi.org/10.4119/unibi/2956041.

ORCID

Gabriele Fischer von Mollard https://orcid.org/0000-0003-3236-1401

REFERENCES

Abdelkafi-Koubaa, Z., Jebali, J., Othman, H., Morjen, M., Aissa, I., Zouari-Kesentini, R., Bazaa, A., Ellefi, A. A., Majdoub, H., Srairi-Abid, N., Gargouri, Y., El Ayeb, M., & Marrakchi, N. (2014). A thermoactive L-amino acid oxidase from Cerastes cerastes snake venom: Purification, biochemical and molecular characterization. *Toxicon*, *89*, 32–44. https://doi.org/10.1016/j.toxicon.2014.06.020

Ahn, M. Y., Ryu, K. S., Lee, Y. W., & Kim, Y. S. (2000). Cytotoxicity and L-amino acid oxidase activity of crude insect drugs. *Archives of Pharmacal Research*, *23*, 477–481. https://doi.org/10.1007/BF02976576

Alexandre, F. R., Pantaleone, D. P., Taylor, P. P., Fotheringham, I. G., Ager, D. J., & Turner, N. J. (2002). Amine-boranes: effective reducing agents for the deracemisation of DL-amino acids using L-amino acid oxidase from Proteus myxofaciens. *Tetrahedron Letters*, *43*, 707–710. https://doi.org/10.1016/S0040-4039(01)02233-X

Bender, A. E., & Krebs, H. A. (1950). The oxidation of various synthetic alpha-amino-acids by mammalian D-amino-acid oxidase, L-amino-acid oxidase of cobra venom and the L-amino-acid and D-amino-acid oxidases of Neurospora crassa. *The Biochemical Journal*, *46*, 210–219.

Bloess, S., Beuel, T., Krüger, T., Sewald, N., Dierks, T., & Fischer von Mollard, G. (2019). Expression, characterization, and site-specific covalent immobilization of an L-amino acid oxidase from the fungus Hebeloma cylindrosporum. *Applied Microbiology and Biotechnology*, *103*, 2229–2241. https://doi.org/10.1007/s00253-018-09609-7

Bretthauer, R. K., & Castellino, F. J. (1999). Glycosylation of Pichia pastoris-derived proteins. *Biotechnology and Applied Biochemistry*, *30*, 193–200. https://doi.org/10.1111/j.1470-8744.1999.tb00770.x

Cheng, C. H., Yang, C. A., Liu, S. Y., Lo, C. T., Huang, H. C., Liao, F. C., & Peng, K. C. (2011). Cloning of a novel L-amino acid oxidase from trichoderma harzianum ETS 323 and bioactivity analysis of over-expressed L-amino acid oxidase. *Journal of Agriculture and Food Chemistry*, *59*, 9142–9149. https://doi.org/10.1021/jf201598z

Derby, C. D., Gilbert, E. S., & Tai, P. C. (2018). Molecules and mechanisms underlying the antimicrobial activity of escapin, an L-amino acid oxidase from the ink of sea hares. *Biological Bulletin*, *235*, 52–61. https://doi.org/10.1086/699175

Geueke, B., & Hummel, W. (2002). A new bacterial L-amino acid oxidase with a broad substrate specificity: Purification and characterization. *Enzyme and Microbial Technology*, *31*, 77–87. https://doi.org/10.1016/S0141-0229(02)00072-8

Hahn, K., Hertle, Y., Bloess, S., Kottke, T., Hellweg, T., & Fischer von Mollard, G. (2017). Activation of recombinantly expressed l-amino acid oxidase from rhizoctonia solani by sodium dodecyl sulfate. *Molecules*, *22*, 2272. https://doi.org/10.3390/molecules22122272

Hahn, K., Neumeister, K., Mix, A., Kottke, T., Gröger, H., & Fischer von Mollard, G. (2017). Recombinant expression and characterization of a L-amino acid oxidase from the fungus Rhizoctonia solani. *Applied Microbiology and Biotechnology*, *101*, 2853–2864. https://doi.org/10.1007/s00253-016-8054-y

Heß, M. C., Bloess, S., Risse, J. M., Friehs, K., & Fischer von Mollard, G. (2020). Recombinant expression of an L-amino acid oxidase from the fungus Hebeloma cylindrosporum in Pichia pastoris including fermentation. *Microbiology Open*, *9*, e1112. https://doi.org/10.1002/mbo3.1112

Isobe, K., & Nagasawa, S. (2007). Characterization of N-alpha-Benzyloxycarbonyl-L-Lysine oxidizing enzyme from Rhodococcus sp AIU Z-35-1. *Journal of Bioscience and Bioengineering*, *104*, 218–223. https://doi.org/10.1263/jbb.104.218

Izidoro, L. F. M., Ribeiro, M. C., Souza, G. R. L., Sant'Ana, C. D., Hamaguchi, A., Homsi-Brandeburgo, M. I., Goulart, L. R., Beleboni, R. O., Nomizo, A., Sampaio, S. V., Soares, A. M., & Rodrigues, V. M. (2006). Biochemical and functional characterization of an L-amino acid oxidase isolated from Bothrops pirajai snake venom. *Bioorganic & Medicinal Chemistry*, *14*, 7034–7043. https://doi.org/10.1016/j.bmc.2006.06.025

Izidoro, L. F. M., Sobrinho, J. C., Mendes, M. M., Costa, T. R., Grabner, A. N., Rodrigues, V. M., da Silva, S. L., Zanchi, F. B., Zuliani, J. P., Fernandes, C. F. C., Calderon, L. A., Stábeli, R. G., & Soares, A. M. (2014). Snake Venom L-Amino Acid Oxidases: Trends in Pharmacology and Biochemistry. *BioMed Research International*, *2014*, 196754. https://doi.org/10.1155/2014/196754

Kasai, K., Ishikawa, T., Komata, T., Fukuchi, K., Chiba, M., Nozaka, H., Nakamura, T., Sato, T., & Miura, T. (2010). Novel L-amino acid oxidase with antibacterial activity against methicillin-resistant Staphylococcus aureus isolated from epidermal mucus of the flounder Platichthys stellatus. *FEBS Journal*, *277*, 453–465. https://doi.org/10.1111/j.1742-4658.2009.07497.x

Kommoju, P. R., Macheroux, P., & Ghisla, S. (2007). Molecular cloning, expression and purification of L-amino acid oxidase from the Malayan pit viper Calloselasma rhodostoma. *Protein Expression and Purification*, *52*, 89–95. https://doi.org/10.1016/j.pep.2006.09.016

Nakano, S., Kozuka, K., Minamino, Y., Karasuda, H., Hasebe, F., & Ito, S. (2020). Ancestral L-amino acid oxidases for deracemization and stereoinversion of amino acids. *Communications Chemistry*, *3*, 181. https://doi.org/10.1038/s42004-020-00432-8

Nakano, S., Minamino, Y., Hasebe, F., & Ito, S. (2019). Deracemization and stereoinversion to aromatic D-amino acid derivatives with ancestral L-amino acid oxidase. *ACS Catalysis*, *9*, 10152–10158. https://doi.org/10.1021/acscatal.9b03418

Niedermann, D. M., & Lerch, K. (1990). Molecular cloning of the L-amino-acid oxidase gene from Neurospora crassa. *Journal of Biological Chemistry*, *265*, 17246–17251. https://doi.org/10.1016/S0021-9258(17)44895-2

Nuutinen, J. T., & Timonen, S. (2008). Identification of nitrogen mineralization enzymes, L-amino acid oxidases, from the ectomycorrhizal fungi Hebeloma spp. and Laccaria bicolor. *Mycological Research*, *112*, 1453–1464. https://doi.org/10.1016/j.mycres.2008.06.023

Pawelek, P. D., Cheah, J., Coulombe, R., Macheroux, P., Ghisla, S., & Vrielink, A. (2000). The structure of L-amino acid oxidase reveals the substrate trajectory into an enantiomerically conserved active site. *EMBO Journal*, *19*, 4204–4215. https://doi.org/10.1093/emboj/19.16.4204

Piedras, P., Pineda, M., Munoz, J., & Cardenas, J. (1992). Purification and characterization of an L-amino-acid oxidase from Chlamydomonas reinhardtii. *Planta*, *188*, 13–18. https://doi.org/10.1007/BF01160707

Pollegioni, L., Motta, P., & Molla, G. (2013). L-Amino acid oxidase as biocatalyst: A dream too far ? *Applied Microbiology and Biotechnology*, *97*, 9323–9341. https://doi.org/10.1007/s00253-013-5230-1

Rodrigues, R. S., da Silva, J. F., Boldrini França, J., Fonseca, F. P. P., Otaviano, A. R., Henrique Silva, F., Hamaguchi, A., Magro, A. J., Braz, A. S. K., & dos Santos, J. I. (2009). Structural and functional properties of Bp-LAAO, a new L-amino acid oxidase isolated from Bothrops pauloensis snake venom. *Biochimie*, *91*, 490–501. https://doi.org/10.1016/j.biochi.2008.12.004

Sabotic, J., Brzin, J., Erjavec, J., Dreo, T., Znidaric, M. T., Ravnikar, M., & Kos, J. (2020). L-amino acid oxidases from mushrooms

show antibacterial activity against the phytopathogen ralstonia solanacearum. *Frontiers in Microbiology*, *11*, 977. https://doi.org/10.3389/fmicb.2020.00977

Scorer, C. A., Clare, J. J., McCombie, W. R., Romanos, M. A., & Sreekrishna, K. (1994). Rapid selection using G418 of high copy number transformants of Pichia pastoris for high-level foreign gene-expression. *Biotechnology*, *12*, 181–184. https://doi.org/10.1038/nbt0294-181

Stábeli, R. G., Marcussi, S., Carlos, G. B., Pietro, R. C. L. R., Selistre-de-Araújo, H. S., Giglio, J. R., Oliveira, E. B., & Soares, A. M. (2004). Platelet aggregation and antibacterial effects of an L-amino acid oxidase purified from Bothrops alternatus snake venom. *Bioorganic & Medicinal Chemistry*, *12*, 2881–2886. https://doi.org/10.1016/j.bmc.2004.03.049

Sun, Y. P., Nonobe, E., Kobayashi, Y., Kuraishi, T., Aoki, F., Yamamoto, K., & Sakai, S. (2002). Characterization and expression of L-amino acid oxidase of mouse milk. *Journal of Biological Chemistry*, *277*, 19080–19086. https://doi.org/10.1074/jbc.M200936200

Wu, S. X., & Letchworth, G. J. (2004). High efficiency transformation by electroporation of Pichia pastoris pretreated with lithium acetate and dithiothreitol. *BioTechniques*, *36*, 152–154. https://doi.org/10.2144/04361DD02

Yang, C. A., Cheng, C. H., Lo, C. T., Liu, S. Y., Lee, J. W., & Peng, K. C. (2011). A novel L-amino acid oxidase from trichoderma harzianum ETS 323 associated with antagonism of Rhizoctonia solani. *Journal of Agricultural and Food Chemistry*, *59*, 4519–4526. https://doi.org/10.1021/jf104603w

Yang, H. C., Johnson, P. M., Ko, K. C., Kamio, M., Germann, M. W., Derby, C. D., & Tai, P. C. (2005). Cloning, characterization and expression of escapin, a broadly antimicrobial FAD-containing L-amino acid oxidase from ink of the sea hare Aplysia californica. *Journal of Experimental Biology*, *208*, 3609–3622. https://doi.org/10.1242/jeb.01795

Yu, Z. L., & Qiao, H. (2012). Advances in non-snake venom L-amino acid oxidase. *Applied Biochemistry and Biotechnology*, *167*, 1–13. https://doi.org/10.1007/s12010-012-9611-1

How to cite this article: Heß, M. C., Grollius, M., Duhay, V., Koopmeiners, S., Bloess, S., & Fischer von Mollard, G. (2021). Analysis of N-glycosylation in fungal L-amino acid oxidases expressed in the methylotrophic yeast *Pichia pastoris*. *MicrobiologyOpen*, 10, e1224. https://doi.org/10.1002/mbo3.1224

APPENDIX

TABLE A1 Overview of used primer for cloning of the LAAOs

Primer	Sequence (5′–3′)	Plasmid	Yeast strain
9His-*nc*LAAO1			
EcoRI_Neurospora_for5	AAGAATTC**CATCATCATCACCATCACCACCAC**CATATGGCTACTAAGCCATCTGACTCCG	pMCH15	MCH13
NotI_Neurospora_rev6	GCGGCCGC**TTA**AACGTCGATC		
9His-*fr*LAAO1			
EcoRI_Fibroporia_for3	AAGAATTC**CATCATCATCACCATCACCACCAC**CATATGCCATCCATTAGAGGT	pMCH21	MCH17
NotI_Fibroporia_rev4	AAGCGGCCGC**TTA**AGCAATGGACTTAGCCT		
9His-*cg*LAAO1			
EcoRI-HC_f3	AAGAATTC**CATCATCATCACCATCACCACCAC**CATATGTCCCAGGTTAGAAGAGAT	pSBL12	MCH5
NotI-HC_r4	AAGGCGGCCGC**TTA**TGGCCAGGA		
9His-*la*LAAO2			
EcoRI_Laccaria_for7	AAGAATTC**CATCATCATCACCATCACCACCAC**CATATGGCTACTGACATCCCATACGACGTT	pMCH13	MCH8
NotI_Laccaria_rev8	GCGGCCGC**TTA**AGCACCGGA		
hc_N54A_fwd1	CTAACACTTTGGGTGAGAAGGCCATCTCTGTTCCATCTT		
hc_N54A_rev1	TGGAGAAGATGGAACAGAGATGGCCTTCTCACCC		
hc_N193A_fwd2	TCCAGCTTTGGGTATCGCCTCCTCCTTGATTGA		
hc_N193A_rev2	GATGTCAATCAAGGAGGAGGCGATACCCAAAGCT		
hc_N331A_fwd3	GGTAACGCTTTCGTTATGGCCGCTTCCGTTACT		
hc_N331A_rev3	ATAGCAGTAACGGAAGCGGCCATAACGAAAGCGTTA		
hc_N164A_for4	ACTACTTCAAGTCCGCCAAGTCCCCAGGTTTC		
hc_N164A_rev4	CTGGAAACCTGGGGACTTGGCGGACTTGAAGT		
EcoRI_for1	AAGAATTCTTCGAAGGATCCAAACGATGAGAT		
Not1-HH_r2	AAGGCGGCCGC**TTA**AACGGAAAC		

Notes: Forward primers: underlined- EcoRI site, bold- 9His-tag.
Reverse primers: underlined- NotI site, bold- stop codon.

TABLE A2 Substrate spectrum of 9His-*cg*LAAO1

	Substrates	Relative activity (%)
Hydrophobic amino acids	L-alanine	70
	ß-alanine	0
	L-isoleucine	4
	L-leucine	90
	L-*tert*-leucine	0
	L-norleucine	99
	L-methionine	64
	L-phenylalanine	65
	L-phenylglycine	0
	rac-β-phenylalanine	0
	L-proline	0
	L-tryptophan	33
	L-valine	3
Polar amino acids	L-asparagine	50
	L-cysteine	0
	L-glutamine	100
	L-serine	5
	L-threonine	0
	L-tyrosine[a]	53
Basic amino acids	L-arginine	37
	L-histidine	17
	L-lysine	41
	L-ornithine	53
Acidic amino acids	L-aspartic acid	3
	L-glutamic acid	21
Amino acid derivates	L-alanine ethyl ester	16
	L-glutamic acid dimethyl ester	33
	L-leucine methyl ester	55
	L-methionine methyl ester	45
	L-phenylalanine methyl ester	32
	L-tyrosine methyl ester	11
	L-threonine methyl ester	0
	L-leucine ethyl ester	35
	L-ß-alanine ethyl ester	0
	L-DOPA[a]	8
	DL-homophenylalanine[a]	77
	4-chloro-DL-phenylalanine	55

Note: $n = 3$.

[a]2.5 mM.

TABLE A3 Kinetic properties of 9His-*cg*LAAO1

	K_m [mM]	v_{max} [U mg^{-1}]	k_{cat} [s^{-1}]	k_{cat}/K_m [s^{-1} mM^{-1}]
L-glutamine	0.76 ± 0.1	12.04 ± 3.6	13.76	18.11
L-leucine	1.20 ± 0.2	9.97 ± 1.0	11.40	9.50
L-leucine methyl ester	12.88 ± 0.3	13.64 ± 0.6	15.59	1.21
L-phenylalanine	0.32 ± 0.03	4.51 ± 0.2	5.15	16.11
L-phenylalanine methyl ester	3.97 ± 0.2	3.41 ± 0.2	3.90	0.98
L-methionine	1.06 ± 0.5	9.84 ± 1.8	11.25	10.61

Note: Data are means of three biological replicas ($n = 3$).

TABLE A4 Substrate spectrum of 9His-*nc*LAAO1

	Substrates	Rel. activity (0.1 mM)	Spec. activity (U mg^{-1}) (0.1 mM)	Spec. activity (U mg^{-1}) (10 mM)
Hydrophobic amino acids	L-alanine	15	0.18 ± 0.006	0.37 ± 0.06
	L-isoleucine	3	0.03 ± 0.002	0.33 ± 0.05
	L-leucine	95	1.09 ± 0.02	0.37 ± 0.07
	L-methionine	61	0.70 ± 0.10	0.14 ± 0.001
	L-phenylalanine	91	1.05 ± 0.02	0.53 ± 0.003
	L-phenylglycine	0	0	0.12 ± 0.02
	L-proline	0	0	0.02 ± 0.02
	L-tryptophan	84	0.96 ± 0.11	0.11 ± 0.06
	L-valine	0	0	0.21 ± 0.04
Polar amino acids	L-asparagine	65	0.75 ± 0.06	0.46 ± 0.05
	L-cysteine	0	0	0
	L-glutamine	63	0.73 ± 0.146	0.37 ± 0.04
	L-serine	0	0	0.29 ± 0.02
	L-threonine	0	0	0.24 ± 0.07
	L-tyrosine	67	0.77 ± 0.10	*0.58 ± 0.23
Basic amino acids	L-arginine	93	1.07 ± 0.03	0.13 ± 0.004
	L-histidine	75	0.86 ± 0.02	0.33 ± 0.06
	L-lysine	54	0.62 ± 0.16	0.08 ± 0.03
Acidic amino acids	L-aspartic acid	0	0	0.50 ± 0.02
	L-glutamic acid	0	0	0.49 ± 0.02
Amino acid derivates	L-leucine methyl ester	20	0.24 ± 0.01	0.89 ± 0.08
	L-phenylalanine methyl ester	17	0.19 ± 0.003	0.94 ± 0.17
	L-leucine ethyl ester	7	0.08 ± 0.007	0.96 ± 0.07
	N-α-acetyl-L-lysine	100	1.15 ± 0.02	0.24 ± 0.05

Note: $n = 3$ ([S] = 0.1 mM/10 mM).

*2.5 mM

TABLE A5 Kinetic properties of 9His-*nc*LAAO1

	K_m [μM]	v_{max} [U mg^{-1}]	k_{cat} [s^{-1}]	k_{cat}/K_m [s^{-1} mM^{-1}]
L-leucine	10 ± 8.6	1.11 ± 0.10	1.18	120
L-leucine methyl ester	610 ± 160	1.09 ± 0.03	1.17	2
L-leucine ethyl ester	70 ± 30	1.23 ± 0.04	1.32	20
L-phenylalanine	7.4 ± 4.7	1.06 ± 0.05	1.13	150
L-phenylalanine methyl ester	50 ± 20	1.07 ± 0.02	1.15	23
L-arginine	5 ± 0.3	1.27 ± 0.07	1.35	270

Note: Data are means of three biological replicas ($n = 3$).

TABLE A6 Effect of N-glycosylation on 9His-*hc*LAAO4 activity

	Untreated [U mg^{-1}]	Activated (pH 3) [U mg^{-1}]
Wt	14.1 ± 4.0	42.8 ± 4.0
+PNGaseF, 37°C	14.5 ± 3.1	40.4 ± 1.5
N54A	4.9 ± 0.7	40.7 ± 3.7
N164A	13.4 ± 3.1	40.0 ± 1.6
N193A	13.1 ± 3.8	41.5 ± 9.6
N331A	13.1 ± 3.4	44.5 ± 4.7
N164A N193A N331A	11.7 ± 2.2	39.6 ± 1.5
ΔN-Glyc.	2.4 ± 0.9	44.5 ± 6.2
E. coli Wt	1.1 ± 0.1	33.0 ± 5.8

Note: Data are means of three biological replicas ($n = 3$) ± standard deviations.

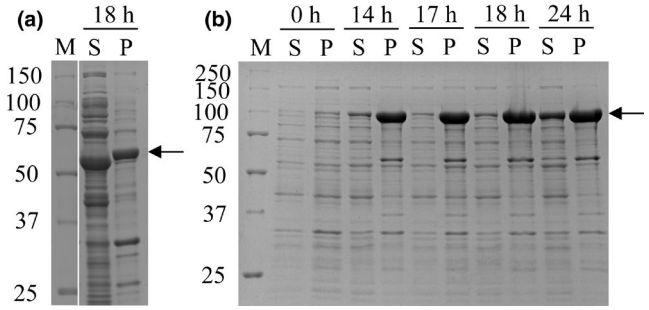

Figure A1 Expression of 6His-*nc*LAAO1 and MBP-*cg*LAAO1 in *E. coli* Arctic Express (DE3). (a) 6His-*nc*LAAO1 (64 kDa) was found only as insoluble protein in the pellet fraction (P) and not in the supernatant (S) after cell lysis. (b) MBP-*cg*LAAO1 was detected predominately in the pellet fraction. The low amounts of the soluble enzyme were inactive. Expression was induced with 0.05 mM IPTG for 18 h (6His-*nc*LAAO1) or the indicated periods (MBP-*cg*LAAO1) at 11°C. Samples were separated by SDS-PAGE and stained with Coomassie Brilliant Blue

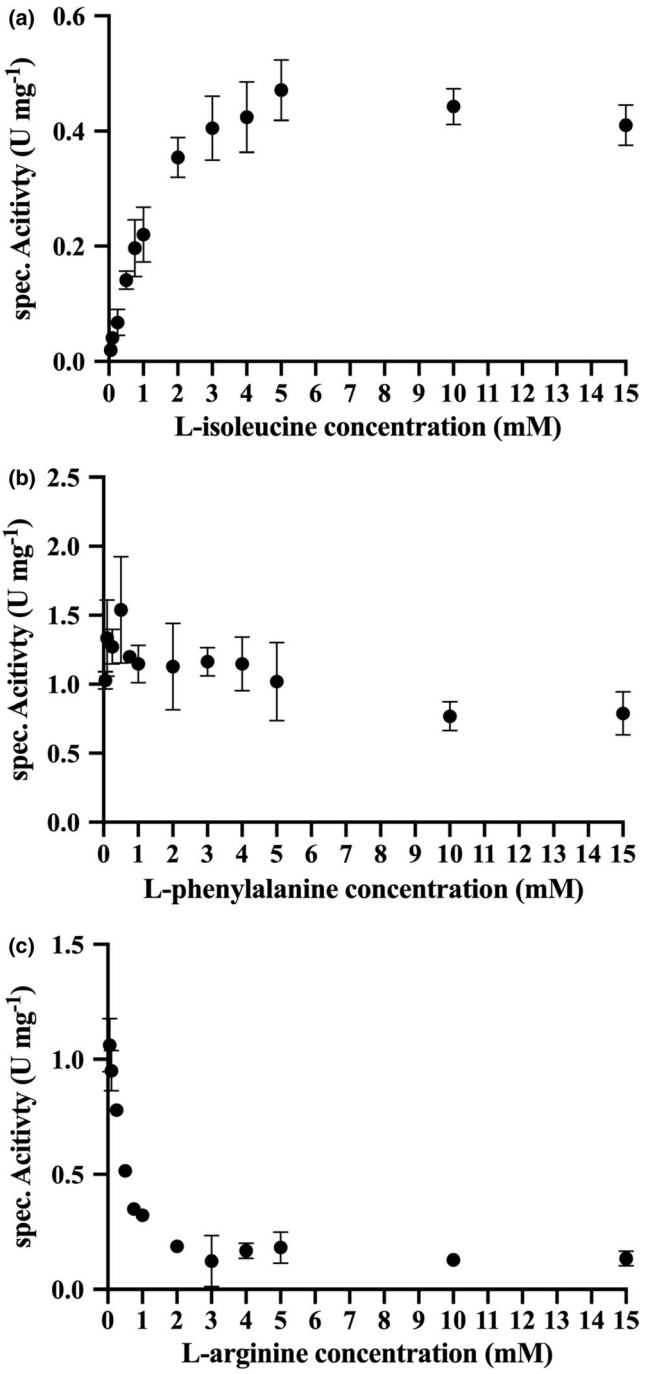

Figure A2 Concentration-dependent activity of 9His-*nc*LAAO1 toward different substrates. Initial activities of the purified enzyme were measured with different substrate concentrations (0.1 mM–15 mM) for (a) L-isoleucine, (b) L-phenylalanine and (c) L-arginine. (a) For L-isoleucine, 9His-*nc*LAAO1 showed regular enzyme kinetics and a K_m value of 1.6 mM. (b) L-phenylalanine concentrations above the K_m value of 7.4 µM did not have a big impact on the activity of 9His-*nc*LAAO1. (c) A strong reduction of activity could be measured with increasing L-arginine concentration starting already at 0.1 mM. The K_m value was 5 µM for L-arginine. Data are means of three independent experiments; error bars represent standard deviations

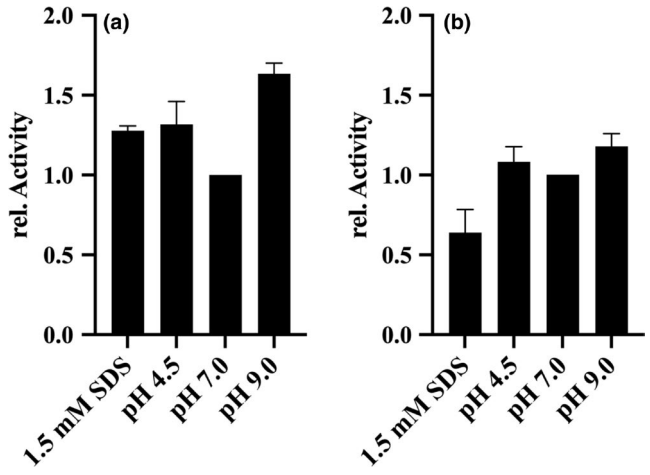

Figure A3 Effect of SDS and pH on the activity of 9His-*nc*LAAO1 and 9His-*cg*LAAO1. The purified LAAOs were preincubated with 1.5 mM SDS or different pH values (4.5, 7.0, or 9.0) for 10 min, and activity was determined with coupled peroxidase and *o*-dianisidine in TEA buffer. The data were normalized to the control incubated at standard conditions (pH 7.0). (a) 9His-*nc*LAAO1 was slightly activated by all tested conditions. (b) The pH treatment of 9His-*cg*LAAO1 showed no impact on activity while 1.5 mM SDS resulted in reduced activity. Data are means of three independent experiments; error bars represent standard deviations